Region-based active contours and sparse representations for texture segmentation

François Lecellier Jalal Fadili Stéphanie Jehan-Besson Marinette Revenu
GREYC UMR CNRS 6072, Caen France
{*firstname.lastname*}*@greyc.ensicaen.fr*

Gilles Aubert
Laboratoire J.A. Dieudonné UMR CNRS 6621, Nice, France
gaubert@math.unice.fr

Abstract

In this paper we propose a rigorous framework for texture image segmentation relying on region-based active contours (RBAC) and sparse texture representation. Such representations allow to efficiently describe a texture by transforming it in a dictionary of appropriate waveforms (atoms) where the texture representation coefficients are concentrated on a small set. For segmentation purposes, these atoms have to be multiscale and localized both in space and frequency, e.g. the wavelet transform. To discriminate different textures, we measure a "distance" between the non-parametric Parzen estimates of their respective sparse-representation coefficients probability density functions (pdfs). These distance measures are then used within RBAC, and we take benefit from shape derivative tools to derive the evolution speed expression of the RBAC. Our framework is applied to both supervised (with reference textures), and unsupervised texture segmentation. A series of experiments on synthetic textures illustrate the potential applicability of our method.

1 Introduction

Texture segmentation remains a difficult challenge and a very active research field. Indeed, the main bottleneck to segment a texture image is to find an appropriate set of generic computable descriptors to characterize a given texture and discriminate distinct textures between them. Representing and characterizing textures remains an important open question, mainly because there is no consensus on how to define a texture, despite many attempts. For instance, Julesz [8] stated simple axioms about the probabilistic characterization of textures. In the literature, there is a flurry of papers devoted to the segmentation of textured images, see e.g. [13, 5, 2, 9, 1]. Some of them attacked the problem of segmenting or classifying textures using the wavelet machinery as texture descriptor [13, 5, 2]. In this paper, we tackle the texture segmentation problem under the umbrella of sparse representations such as, but not limited to, wavelets, and region-based active contours (RBAC). RBAC allows the introduction of region informations to classical active contours [15, 4]. More precisely, we propose a general texture segmentation framework that discriminates textures by measuring a distance between the non-parametric Parzen estimates of their respective sparse-representation coefficients probability density functions (pdfs). The framework is adapted to both supervised and unsupervised segmentation of textured images. In the supervised case, we consider the minimization of a distance between the coefficients pdf of a reference texture, and the one of the texture to segment. In the unsupervised case, we maximize the Kullback-Leibler Divergence (KLD) between the coefficients pdfs.

The paper is organized as follows: Section 2 deals with sparse-representation texture description. The core of our contribution lies in Section 3 where we present the RBAC model and the Parzen pdf estimator-based segmentation method. For illustrative purposes, in Section 4 we provide and discuss some experimental results.

2 Sparse-representation texture descriptor

Many methods exist to characterize a texture, but in the current state of research none is well adapted for all textures. Furthermore, sparsely representing textures remains an open problem. It has been known for some time now that some transforms can sometimes enjoy reasonably sparse expansions of certain textures; e.g. locally oscillatory textures in bases such

as local discrete cosines [12], brushlets [11], Gabor [10], WaveAtoms [14]. Gabor and dyadic traditional wavelets are widely used in the image processing community for texture analysis. Their use may be motivated by physiological evidence where simple cells of the primary visual cortex exhibit Gabor-like responses. But little is known on the decay, hence the sparsity behaviour, of wavelet coefficients of texture in general.

Our goal here is to segment textures in images without confining ourselves to a specific representation to characterize them. Thus, our framework targets representations which are able to discriminate textures while satisfying two major requirements:

- Multiscale, localization and affine invariance (to translation and rotation). We here assume that a texture $u(\mathbf{x})$ has the following linear expansion,

$$u(\mathbf{x}) = \sum_s \sum_b \sum_k \boldsymbol{\alpha}_\gamma(\mathbf{x}) \psi_\gamma(\mathbf{x}) \ , \qquad (1)$$

  where $\gamma = (s, b, k)$, s stands for the scale, b the band or orientation and k the translation parameter. $\boldsymbol{\alpha}_\gamma(\mathbf{x}) = \langle u, \psi_\gamma \rangle$, the representation coefficient. $\psi_\gamma(\mathbf{x})$ are the elementary building atoms well localized in space and frequency, e.g. dilated and translated versions of the mother wavelet in case of the wavelet transform. The term u designs the image intensity inside the textured region.

- Compressibility : we consider representations that are able to (almost) sparsely represent the textures at hand. That is, most of the transform coefficients of these textures vanish and only a few of them are significant [10]. Put formally, the coefficients sorted in descending order of magnitude $|\boldsymbol{\alpha}|_{(i)}$ should satisfy $|\boldsymbol{\alpha}|_{(i)} = O(|i|^{1-2/p})$, $p < 2$, which in turn reflects the fast decay of the non-linear approximation error of the texture with its i highest representation coefficients [10] .

3 Histogram-based segmentation in active contours

There are two major ways to estimate the pdf of a random variable from its finite-sample histogram: non-parametric or parametric. In this paper we focus our attention on non-parametric kernel density estimators. We consider that there is a feature of the image named $\boldsymbol{\alpha}_\gamma \in \chi$, where $\chi \subseteq \mathbb{R}$. We call $q(\boldsymbol{\alpha}_\gamma, \Omega)$ the pdf of $\boldsymbol{\alpha}_\gamma$ inside a region Ω. We can estimate the pdf of $\boldsymbol{\alpha}_\gamma$ using the Parzen method [3, 7].

Let $p : \mathbb{R}^m \rightarrow \mathbb{R}^+$ be the Parzen window, a smooth positive function whose integral is equal to 1. For the sake of simplicity but without loss of generality, we assume that p is an m-dimensional Gaussian with zero-mean and variance σ^2,

$$p(\boldsymbol{\alpha}_\gamma) = g_\sigma(\boldsymbol{\alpha}_\gamma) = \frac{1}{(2\pi\sigma^2)^{1/2}} \exp(-\frac{|\boldsymbol{\alpha}_\gamma|^2}{2\sigma^2}),$$

and we define at a given γ

$$\hat{q}(\boldsymbol{\alpha}_\gamma, \Omega) = \frac{1}{|\Omega|} \int_\Omega g_\sigma(\boldsymbol{\alpha}_\gamma(\mathbf{x}) - \boldsymbol{\alpha}_\gamma) \, d\mathbf{x},$$

where $\boldsymbol{\alpha}_\gamma(\mathbf{x})$ is the value of the feature of interest at the point $\mathbf{x}$ of Ω.

We now assume that we have a function $\Psi : \mathbb{R}^+ \times \mathbb{R}^+ \rightarrow \mathbb{R}^+$ which allows us to compare two pdfs. This function is small if the pdfs are similar and large otherwise. It allows us to introduce the following functional which represents the "distance" between the current pdf estimate $\hat{q}_1(\boldsymbol{\alpha}_\gamma, \Omega)$ and another one $\hat{q}_2(\boldsymbol{\alpha}_\gamma)$:

$$D_\gamma(\Omega) = \int_\chi \Psi \left(\hat{q}_1(\boldsymbol{\alpha}_\gamma, \Omega), \hat{q}_2(\boldsymbol{\alpha}_\gamma) \right) \, d\boldsymbol{\alpha} \qquad (2)$$

We then search for the domain Ω that minimizes:

$$D(\Omega) = \sum_s \sum_b \sum_k D_\gamma(\Omega) \qquad (3)$$

Introducing an initial domain Γ_0, we make it evolve using a shape gradient descent. Using the tools developed in [6], we first compute the Gâteaux derivative of the functional D_γ, to compute the velocity, which leads to the following theorem.

Theorem 1 *The Gâteaux derivative in the direction* $\mathbf{V}$ *of the functional* D_γ *defined in (2) is:*

$$\begin{aligned} < D'_\gamma(\Omega), \mathbf{V} > \ &= \ -\frac{1}{|\ \Omega\ |} \int_\Gamma \Big(\partial_1 \Psi(\hat{q_1}(.), \hat{q_2}(.)) \\ &* \ g_\sigma(\boldsymbol{\alpha}_\gamma(\mathbf{x})) - C(\Omega) \Big) (\mathbf{V} \cdot \mathbf{N}) d\mathbf{a}(\mathbf{x}) \, , \end{aligned}$$

where $C(\Omega) = \int_\chi \partial_1 \Psi(\hat{q}_1(.), \hat{q}_2(.)) \hat{q}_1(.) \, d\boldsymbol{\alpha}$, $*$ *denotes the convolution product,* $\partial_1 \Psi(.,.)$ *the partial derivative of* $\Psi(r,.)$ *according to the first variable* r, Γ *is the boundary of* Ω *and* $\mathbf{N}$ *the unit inward normal to* Γ.

3.1 Supervised texture segmentation

Let us note Ω_{in} the inside region, Ω_{out} the outside region and Γ the interface between the two regions. We search for the partition $\{\Omega_{in}, \Omega_{out}, \Gamma\}$ that minimizes $(D(\Omega_{in}) + D(\Omega_{out}))$ where D is defined in (3).

Using the results of [7] and Theorem 1 we obtain:

Corollary 1 *The evolution speed of the RBAC for the minimization of* $(D(\Omega_{in}) + D(\Omega_{out}))$ *is*

$$\begin{aligned}\frac{\partial \Gamma}{\partial \tau} &= \sum_s \sum_b \sum_k \Big(D_\gamma(\Omega_{in}) - D_\gamma(\Omega_{out}) \\ &+ C(\Omega_{out}) - C(\Omega_{in}) \\ &+ V_{in} * g_\sigma(\boldsymbol{\alpha}_\gamma(\mathbf{x})) - V_{out} * g_\sigma(\boldsymbol{\alpha}_\gamma(\mathbf{x})) \Big) \mathbf{N} \end{aligned} \quad (4)$$

where $\mathbf{N}$ *in the unit inward normal to* Γ*,*

D_γ can be for example the Hellinger distance between an estimated pdf $\hat{q}$ and a reference one $\hat{q}_{ref}$ with:

$$\Psi(\hat{q}(\boldsymbol{\alpha}_\gamma, \Omega), \hat{q}_{ref}(\boldsymbol{\alpha})) = \left(\sqrt{\hat{q}(.)} - \sqrt{\hat{q}_{ref}(.)} \right)^2 .$$

$$C(\Omega) = \int_\chi \frac{\sqrt{\hat{q}(\boldsymbol{\alpha}_\gamma, \Omega)} - \sqrt{\hat{q}_{ref}(\boldsymbol{\alpha}_\gamma)}}{\sqrt{\hat{q}(\boldsymbol{\alpha}_\gamma, \Omega)}} d\boldsymbol{\alpha},$$

$$V(\boldsymbol{\alpha}) = \frac{\sqrt{\hat{q}(\boldsymbol{\alpha}_\gamma, \Omega)} - \sqrt{\hat{q}_{ref}(\boldsymbol{\alpha}_\gamma)}}{\sqrt{\hat{q}(\boldsymbol{\alpha}_\gamma, \Omega)}}.$$

3.2 Unsupervised texture segmentation

When considering the segmentation of an image into two regions Ω_{in} and Ω_{out}, we propose here to consider the maximization of the Kullback-Leibler Divergence (KLD) defined as follows:

Definition 1 *The relative entropy between the pdf estimates* $\hat{q}_{in}(\boldsymbol{\alpha}_\gamma, \Omega_{in})$ *and* $\hat{q}_{out}(\boldsymbol{\alpha}_\gamma, \Omega_{out})$ *of the feature* $\boldsymbol{\alpha}$ *within the regions* Ω_{in} *and* Ω_{out} *is defined as follows:*

$$D_\gamma(\hat{q}_{in} \| \hat{q}_{out}) = \int_\chi \hat{q}_{in}(\boldsymbol{\alpha}, \Omega_{in}) \log \left(\frac{\hat{q}_{in}(\boldsymbol{\alpha}, \Omega_{in})}{\hat{q}_{out}(\boldsymbol{\alpha}, \Omega_{out})} \right) d\boldsymbol{\alpha} . \quad (5)$$

which is always positive, convex but non-symmetric.

The KLD-maximization based segmentation criterion will look for the configuration that maximizes the log-likelihood of the data $\boldsymbol{\alpha}$ under their actual model $\hat{q}_{in}$, while minimizing the plausibility of the same data under $\hat{q}_{out}$. Thus, translating this into a segmentation setting, the KLD acts as a region competition criterion.

As stated above, KLD is a non-symmetric quantity, that is to say it does not give the same weight to inside and outside region. We then propose to use a symmetric description to express KLD which corresponds to the functional D_γ defined in (2) using:

$$\Phi(\hat{q}_{in}, \hat{q}_{out}) = \frac{D(\hat{q}_{in} \| \hat{q}_{out}) + D(\hat{q}_{out} \| \hat{q}_{in})}{2} . \quad (6)$$

We derive the evolution speed of the RBAC for (6):

Corollary 2 *The evolution speed of the RBAC in the case of KLD maximization is:*

$$\begin{aligned}\frac{\partial \Gamma}{\partial \tau} &= \sum_s \sum_b \sum_k \Big(\frac{1}{2|\Omega_{in}|} (V_{in} * g_\sigma(\boldsymbol{\alpha}_\gamma(\mathbf{x})) - C_{in}) \\ &+ \frac{1}{2|\Omega_{out}|} (V_{out} * g_\sigma(\boldsymbol{\alpha}_\gamma(\mathbf{x})) - C_{out}) \Big) \mathbf{N} \end{aligned} \quad (7)$$

where $\mathbf{N}$ *in the unit inward normal to* Γ*,*

$$C_{in} = \int_\chi \frac{1}{2} \hat{q}_{in} \Big(1 - \frac{\hat{q}_{in}}{\hat{q}_{out}} + \log(\frac{\hat{q}_{out}}{\hat{q}_{in}}) \Big) d\boldsymbol{\alpha}$$

$$V_{in}(\boldsymbol{\alpha}) = \frac{1}{2} \left(1 - \frac{\hat{q}_{in}(\boldsymbol{\alpha})}{\hat{q}_{out}(\boldsymbol{\alpha})} + \log \left(\frac{\hat{q}_{out}(\boldsymbol{\alpha})}{\hat{q}_{in}(\boldsymbol{\alpha})} \right) \right)$$

C_{out} *and* V_{out} *are the exact symmetric of* C_{in} *and* V_{in}*.*

4 Experimental results

In the following experiments, we considered that our texture can be sparsified by the undecimated wavelet transform (UDWT). This wavelet decomposition is translation-invariant and gives three bands at each scale. To segment homogeneous textured regions, we have to aggregate the wavelet responses at all scales and bands. Obviously, our segmentation algorithm will perform well if the textures are well discriminated by the UDWT. We do not present other transforms due to the lack of enable space in the paper. In all the experiments we add, to the evolution speed, a classical regularization term chosen as the curvature and balanced with a positive real integer $\lambda = 10$. The initial curve is chosen as a set of bubbles disposed on the whole images and the computation time is less than one minute on a 3.0 GHz Itanium processor.

4.1 Supervised segmentation

Here, we used an image with reference textures to learn their statistical properties. Our experimental study was carried out in two steps. First, we computed the wavelet transform coefficients of the reference image, and estimated their pdfs for each texture (region) at each scale and band. The image to segment is composed of the same textures as the reference but at different locations (Fig.1 a, b). Second, the estimated reference pdfs were plugged in (4) to compute the evolution speed of the evolving contour(s).

The segmentation results are depicted in Fig.1 (c), (d). Visually, we can see that our segmentation is very close to the true image partition. Quantitatively, we computed the False Classification Rate (FCR) for each image. In Fig.1 (c), this rate is 1.26%. This can be explained by the fact that the UDWT is good at sparsifying the vertically oscillating textures. On the textures of Fig.1 (b)-(d), the FCR is 5.48%. This is intuitively

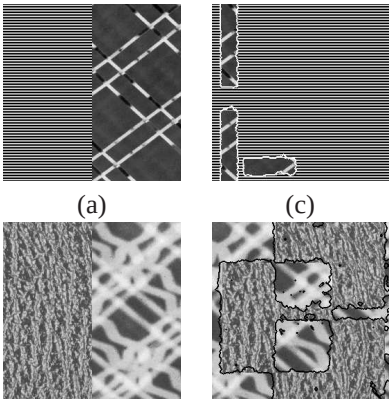

Figure 1. (a-b) Reference images to learn UDWT coefficients pdfs, (c-d) Segmented images using (4).

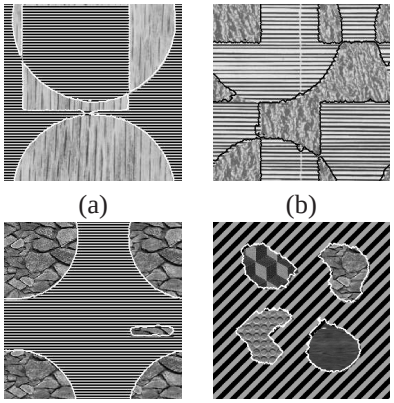

Figure 2. Unsupervised KLD-based segmentation.

acceptable as the two textures are not very well sparsified by the UDWT. An additional reason for this higher FCR on this image is that as we use the level sets implementation of active contours, the thin regions (on the right) are difficult to capture, hence inflating the FCR.

4.2 Unsupervised KLD-based segmentation

In this case, as explained in Section 3.2, we aim at maximizing the KLD between inside and outside pdf estimates. The four images are well segmented and composed of two (or more) textures, where at least one texture in each image is well sparsified by the UDWT (Fig.2). For the image in Fig.2 (a), the FCR=2.35%. The two textures composing the image are sparsely represented by wavelets because they are essentially oscillatory patterns with main horizontal and vertical orientations. For Fig.2 (b), the FCR is 3.53%, this is quite low considering the poor sparsification of one of the two textures. The example of Fig.2 (c) gives FCR=1.60% given that the UDWT is a good sparse representation of these textures, and the simple partition of the image. We present results for more than two textures on image Fig.2 (d) , to show that our method is not restricted to the segmentation of only two regions. Our method does a very good job at segmenting the different textures, without the need of a reference, with a FCR=2.28%. However, one has to keep in mind that this was possible because the outside texture (here diagonally oscillating) is efficiently sparsified by the UDWT, which makes it easily discernible from the other textures.

References

[1] M. Alemán-Flores, L. Álvares, and V. Caselles. Texture-oriented anisotropic filtering and geodesic active contours in breast tumor ultrasound segmentation. *J. Math. Imaging Vis.*, 81–97, 2007.

[2] J.-F. Aujol, G. Aubert, and L. Blanc-Féraud. Wavelet-based level set evolution for classification of textured images. *IEEE Trans. IP*, 1634–1641, 2003.

[3] P. Bickel and K. Docksum. *Mathematical statistics: basic ideas and selected topics*, Prentice-Hall, 2001.

[4] V. Caselles, R. Kimmel, and G. Sapiro. Geodesic active contours. *IJCV*, 22:61–79, 1997.

[5] M. N. Do and M. Vetterli. Wavelet-based texture retrieval using generalized gaussian density and kullback-leibler distance. *IEEE Trans. IP*, 146–158, 2002.

[6] S. Jehan-Besson, M. Barlaud, and G. Aubert. Dream2s: Deformable regions driven by an eulerian accurate minimization method for image and video segmentation. *IJCV*, 45–70, 2003.

[7] S. Jehan-Besson, M. Barlaud, and G. Aubert. Shape gradients for histogram segmentation using active contours. In *ICCV*, 2003.

[8] B. Julesz. Visual pattern discrimination. *RE Trans. Inform. Theory*, 84–92, 1962.

[9] I. Karoui, R. Fablet, J. M. Boucher, and J. M. Augustin. Region-based image segmentation using texture statistics and level-set methods. In *ICASSP*, 2006.

[10] S. Mallat. *A Wavelet tour of signal processing*. Academic Press, 1998.

[11] F. G. Meyer and R. R. Coifman. Brushlets: a tool for directional image analysis and image compression. *App. Comp. Harm. Anal.*, 147–187, 1997.

[12] J. L. Starck, M. Elad, and D. L. Donoho. Redundant multiscale transforms and their application for morphological component analysis. *AIEP*, 2004.

[13] M. Unser. Texture classification and segmentation using wavelet frames. *IEEE Trans. IP*, 1549–1560, 1995.

[14] L. Ying and L. Demanet. Wave atoms and sparsity of oscillatory patterns. *App. Comp. Harm. Anal.*, 368–387, 2007.

[15] S. Zhu and A. Yuille. Region competition: unifying snakes, region growing, and bayes/MDL for multiband image segmentation. *IEEE PAMI*, 884–900, 1996.